EasyChair Preprint

№ 13123

Structural Behavior and Low Cycle Fatigue Characteristics of Suspension Support Member for Building Equipment

Ichiro Hirano, Shoichi Kishiki and Miku Kurosawa

April 28, 2024

Structural Behavior and Low Cycle Fatigue Characteristics of Suspension Support Member for Building Equipment

Ichiro Hirano[1][0000-0002-9803-2427], Shoichi Kishiki[2][0000-0002-9645-7851], and Miku Kurosawa[3][0000-0002-5961-4328]

[1] Doctoral Student, Tokyo Institute of Technology, Kanagawa, Japan
[2] Assistant Professor, Tokyo Institute of Technology, Dr. Eng., Kanagawa, Japan
[3] Professor, Tokyo Institute of Technology, Dr. Eng., Kanagawa, Japan
hirano.i.ab@m.titech.ac.jp

Abstract. The installation method for earthquake-resistant support of suspension equipment such as air-conditioners is generally to connect braces to the hanging bolts via mounting hardware. However, it has been reported that hanging bolt, which is one of the members supporting suspension equipment (suspension support members), has been cyclically deformed during earthquakes, resulting in fractures at the suspension source. The fall of the equipment due to the fracture of suspension support members is a serious damage that directly leads to the loss of building functions. In this study, Cyclic loading tests were conducted to investigate the structural behavior and low cycle fatigue (LCF) characteristics of suspension support members.

The test specimens consist of four hanging bolts, each side of which is reinforced by X-shaped braces. The main test parameters are the suspension length and the angle of the brace. Cyclic loading applying the forced deformation to the suspension side of the hanging bolts was conducted until either the hanging bolt fracture or significant damage in other parts of the specimens.

In evaluating the initial stiffness and the yield strength of the suspension support members, considering the effect of the mounting hardware, both were evaluated well under the current recommended specifications for seismic support. And then, the test result showed that the LCF characteristics of suspension support members can be evaluated by using the deformation angle at the protrusion, regardless of the presence or absence of bracing.

Keywords: Building equipment, Hanging bolt, Seismic design, Low cycle fatigue characteristics, Miner's law.

1 Introduction

The seismic damage to building equipment is concentrated at the attachment parts to the structural frame and the connections between equipment. Non-structural components including equipment, tend to account for a higher proportion of construction costs than structural frames. Since non-structural components including equipment tend to

account for a higher proportion of construction costs than the structural ones [1], the cost of repairing equipment is considered to be relatively large in post-earthquake restoration. In addition, falling or damaging air-conditioning equipment due to fracture of hanging bolts [2], [3], [4], is a serious damage that directly leads to loss of building functions and human suffering.

The current guideline for seismic design of building equipment [5], states "it is sufficient to ensure seismic support of light equipment weighing 1kN or less by a method specified by a manufacturer of the equipment". However, many manufacturers of equipment do not provide seismic support methods for light weight equipment. References [4], [5], [6], propose the specifications for seismic support of equipment weighing 1kN or less. An example of seismic support for seismic support for air-conditioning equipment is shown in Fig. 1. When supporting equipment with hanging bolts, two braces are placed in an X-shape on each of the four sides of the four hanging bolts. The attachment angle of the braces to the hanging bolts should be within 45±15°, and the total length of the upper protrusion part and the lower protrusion part should not exceed 25cm. The braces are made of a metal material (full thread bolt) of equal or greater strength than the hanging bolts, and the member that fastens the hanging bolt to the brace should be a mounting hardware.

Fatigue fracture of hanging bolts supporting equipment, which is caused by cyclic deformation, has been investigated in previous studies [7], [8], [9]. However, the effects of relatively small amplitude ranges and differences in suspension length and nominal diameters on fatigue characteristics are not clear. The seismic design [6], for equipment attachments presents the concept of structural calculation, but there is no evidence based on structural experiments or numerical analysis.

In this study, cyclic loading tests were conducted to investigate the horizontal stiffness, strength, and low cycle fatigue characteristics of the unit consisting of hanging bolts, braces, and the mounting hardware that fastens them (hereinafter referred to as "suspension support members"), which supports equipment using the attachment angle of braces and the length of hanging bolts as main parameters.

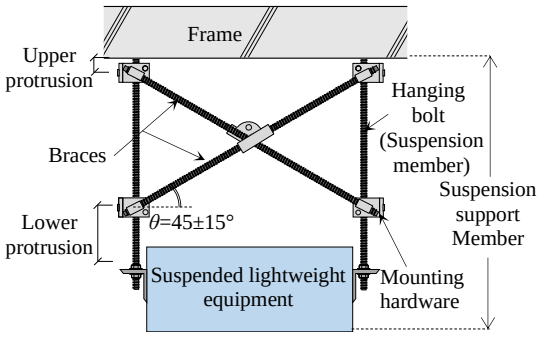

The specification for seismic support of suspended equipment weighting 1kN or less

1. Principle, hanging bolts should be fixed to the frame using insert hardware.
2. Braces with full threaded bolts should be placed on X-shape or radically on all four sides.
3. The angle θ at which the braces is attached to hanging bolts should be $45 \pm 15^{\circ}$ degrees.
4. Braces should be used of metal material of equal or greater strength than hanging bolts.
5. Mounting hardware is used to fasten the hanging bolts to the brace.
6. The total length of the upper and lower protrusion should not exceed 25cm.
7. If the function is to be secured, shaped steel should be used for the suspension members.

Fig. 1. Example of placing the braces of full thread bolts on X-shape for suspended equipment.

2 Test Plan

2.1 Outline of Specimen

The outline of the test specimen is shown in Fig. 2. The test specimen is the suspension support members consisting of four hanging bolts and braces for reinforcing them. Four hanging bolts are placed at intervals of 900mm x 208mm, and support a steel plate (weighing about 0.65kN), which assumed to be lightweight equipment with nuts. The thickness of the steel plates was set so that the in-plane and out-of-plane deformation of the plates is sufficiently small relative to the magnitude of the forced deformation of the suspension support members.

The outline of the mounting hardware used in the tests is shown in Fig. 3. The hanging bolt and braces are connected by angle-shaped mounting hardware. The hanging bolt is fixed by tightening the bolts attached to the mounting hardware with a torque value of 24.5Nm. The attachment angle of the braces can be freely adjusted. The hanging bolt and brace materials used in the tests are full threaded bolts equivalent to SS400, and are basically used on wit screws that are commonly used for seismic support of equipment. Table 1 shows the material properties of the full-thread bolts used in the tests. In the table, E is Young's modulus, G is the shear modulus and σ_y is the yield stress obtained from tensile tests [10]. D_e is the effective diameter of the bolt, which sectional secondary moment I, section modulus, Z, and plastic section modulus, Z_p, were calculated based on test results obtained from three-point bending tests [10].

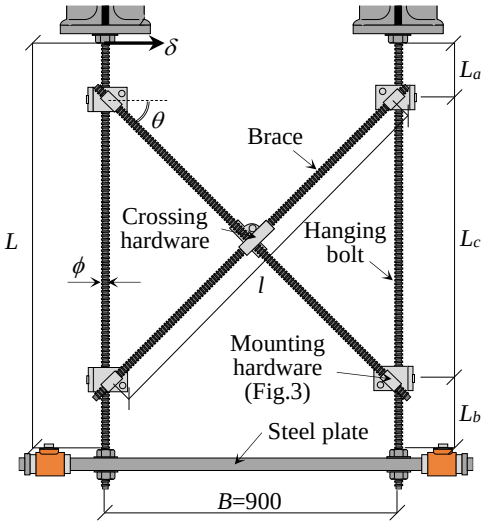

Fig. 2. Outline of specimen.

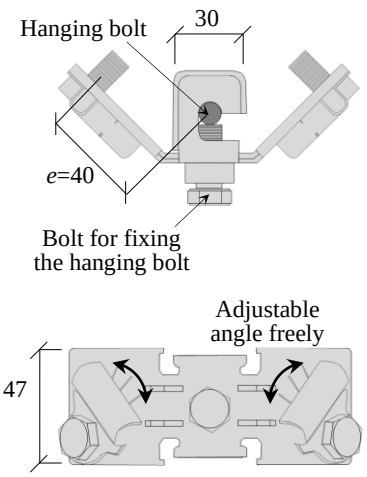

Fig. 3. Outline of mounting hardware.

Table 1. Material properties of full thread bolt (W3/8).

D_e [mm]	A [mm^2]	E [N/mm^2]	G [N/mm^2]	σ_y [N/mm^2]	I [mm^4]	Z [mm^3]	Z_p [mm^3]
7.906	49.1	205000	79000	503.87	125.23	50.80	78.40

2.2 Test parameter

The test parameters for the specimens are shown in Fig. 4. The test parameters are the attachment angle of the brace θ, the upper protrusion length L_a or lower protrusion length L_b from the edge of the brace ends, and the loading amplitude δ. There are four types of attachment angle of brace: 15°, 30°, 45°, and 60°. In general, the upper and lower parts of suspension support members must protrude from the edge of the brace to connect with the air-conditioning equipment or ceiling surface. In this paper, the longer protrusion is defined as the protrusion length L_f. In other words, the protrusion length L_f can be expressed as following.

$$L_f = \max\{L_a, L_b\} \tag{1}$$

There are four types of protrusion length: 100, 250, 400, and 550 mm. The shorter protrusion length is 50 mm for construction convenience. Reference [11], shows the results of cyclic loading tests of only hanging bolts simulating the protrusion of the suspension support members. Based on the fact that the nominal diameter of the hanging bolts φ had a small effect on the low cycle fatigue characteristics, but the suspension length L had a large effect on the low cycle fatigue characteristics, the nominal diameters used for the hanging bolt and brace in the cyclic loading tests of the suspension support members in this paper are all W3/8.

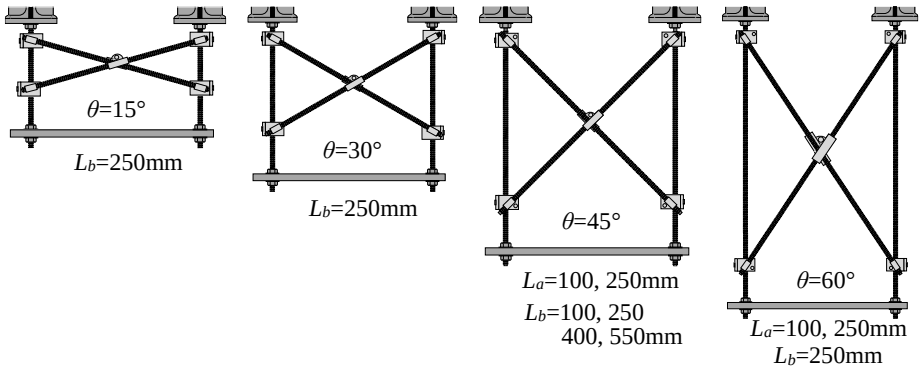

Fig. 4. Test parameters.

2.3 Test setup and measuring plan

The test setup is shown in Fig. 5. The test setup consists of a loading frame, an actuator, and a test specimen. The loading frame is supported by four columns with pin connected to the upper and lower ends, and can move freely in the horizontal direction. The actuator is connected to the middle of the column on one side of the load frame. The test specimen is fixed between the loading frame and the reaction frame and is subjected to forced deformation on the suspension side. The displacement given by the actuator is amplified to 2125/425 (= 5.0 times) and given to the specimen. The hanging bolts are passed through the gap between symmetrically adjacent groove beams, and plates are

installed on the upper and lower flanges of them to tighten the hanging bolt from the upper and lower directions with nuts.

Next, the measurement plan is described. During loading, the horizontal load Q is measured by a load cell attached to the steel plate. The deformation of the specimen is measured from the difference between the absolute displacement at the top end (x_1) and the absolute displacement at the bottom end (x_0) of the suspension support member. In addition, the relative displacement (δ_a or δ_b) of the upper or lower protrusion is measured directly from the displacement transducers (x_2~x_5) attached on the steel plate.

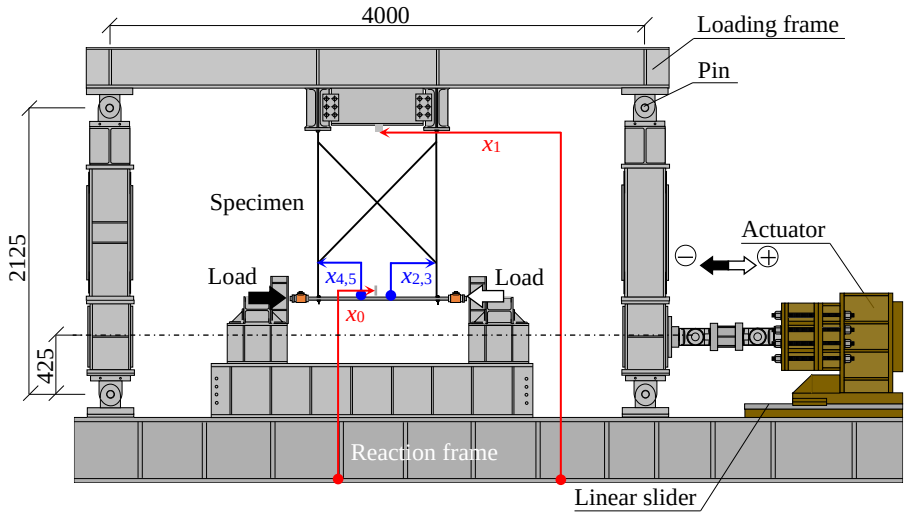

Fig. 5. Test parameters.

2.4 Loading Method

The loading method is described. The test was conducted by applying a constant displacement amplitude cyclic positive-negative cyclic loading as a sinusoidal wave, with the side where the actuator is in tension as the positive side. The loading speed was set so that the maximum velocity given to the specimen was less than 10 mm/s. The loading was continued until the fracture of the hanging bolt was confirmed or until a sudden loss of strength occurred due to significant damage in other parts of the hanging bolts.

3 Low Cycle Fatigue Characteristics

In this chapter, low cycle fatigue characteristics of suspension support members is evaluated. The low cycle fatigue characteristics of suspension support members obtained from cyclic loading test under constant amplitude is examined.

3.1 Cyclic loading test under constant amplitude (fractured of hanging bolts)

N_f is defined as the number of fractures when one of the four hanging bolts fractures or when the maximum strength per cycle of the suspension support member drops to almost half of the maximum strength exerted up to that point, whichever is smaller. The deformation angle R is defined as the ratio of one-sided amplitude δ to the length L_f. The relationship between the number of fractures N_f and the deformation angle $R(=\delta/L_f)$ is shown in Fig. 6. The vertical axis represents the number of fractures, and the horizontal axis represents the deformation angle. Fig. 6(a) shows the case without braces (only hanging bolts), and Fig. 6(b) and (c) show the case with braces, separately for the lower protrusion and upper protrusion, respectively. In each Figure, the specimens that fractured in the calculated elastic range are shown as filled plots and those that fractured in the calculated inelastic range are shown as white plots. In both cases, the number of fractures decreases linearly on both logarithmic axes as the deformation angle increases, results based on the Manson-Coffin law [12]. The straight line in the figure is the fatigue curve for only hanging bolts of L_f=300mm (without braces), and the fatigue curve equation is shown in following equation.

$$N_f = 0.2069R^{-3.059} \tag{2}$$

In the case without braces (Fig. 6(a)), as the suspension length L_f increases, the number of fractures N_f increases for the same deformation angle R. This is thought to be due in part to the fact that the amount of plastic deformation becomes relatively small for the same amplitude as the suspension length L_f increases.

The results of this test are compared with those of the previous one, [7], (○ in Fig. 6(a)). The slope of the fatigue curve in the previous test is slightly steeper than that in this test, and the number of fractures is higher for the same deformation angle. However, when compared with L_f=900 mm, which is almost equal to the length of the previous test (L_f=800 mm), the result of the previous test shows the same number of fractures as those of this test, which confirms the validity of the results of this test.

Next, Fig. 6(b) shows the relationship between the number of fractures N_f and the deformation angle R_b, showing only the specimen, which fractured in the hanging bolt at the lower protrusion part. The lower protrusion length L_b=250mm shows the same fatigue characteristics as that of L_f=300mm without braces (only hanging bolts), whose lengths are almost equal, regardless of the difference in the attachment angle of the

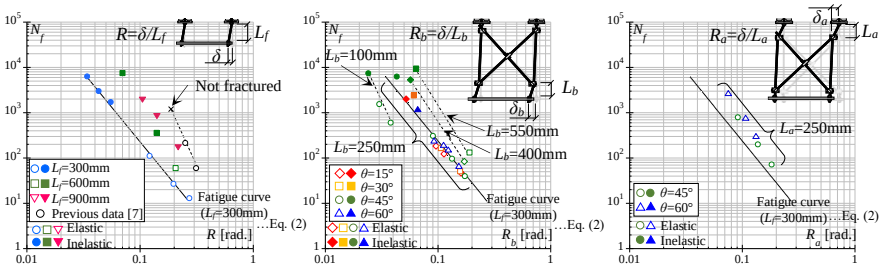

(a) Non-Braced (b) Braced (lower protrusion) (c) Braced (upper protrusion)

Fig. 6. Low-cycle fatigue characteristics (only shown in case of fracture of hanging bolt)

brace (◇□○△ in the graph). As in the case without braces, the number of fractures N_f increases as the suspension length increases (◇□ in the graph). Therefore, it is concluded that the fatigue characteristics can be evaluated by using the deformation angle at the protrusion part as well as without braces.

Finally, Fig. 6(c) shows the relationship between the number of fractures N_f and the deformation angle R_a, showing only the specimen, which fractured in the hanging bolt at the upper protrusion part where axial force is generated. In the case of the upper protrusion (Fig. 6(c)), where axial force is generated, the number of fractures N_f is higher for the same deformation angle R_a than that of a specimen without braces (only hanging bolts) of approximately equal length (L_f=300mm) (○△ in the graph). This is thought to be partly due to the loosening of the threaded part when the tensile axial force acts on the upper protrusion. Therefore, in the axial force range covered here (axial force ratio: 0.2~6.3% in this test), it can be concluded that the low cycle fatigue characteristics of the suspension support members is not reduced.

3.2 Examination of the low-cycle fatigue characteristics cy the different length

Next, the effect of difference in suspension length on the number of fractures is discussed. Fig. 7(a) shows the case without the braces, and Fig. 7(b) shows the case with the braces. The notation in the figures is the same as in the previous section. The straight line in the figure is the fatigue curve for the hanging bolt of L_f=300mm (without braces).

$$N_f = 454.03\mu^{-3.059} \tag{3}$$

Here, the plasticity factor μ is calculated by the following equation.

$$\mu = R/R_p \tag{4}$$

R_p is the calculated value of elastic deformation at the full plastic strength. The value is calculated from the following equation, assuming plastic hinges at the upper and lower ends of the fixed beams at both ends (Fig. 8).

$$R_p = \frac{Q_p}{K_f \cdot L_f} \tag{5}$$

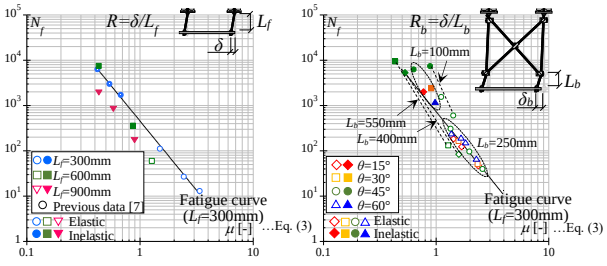

(a) Non-Braced (b) Braced (lower protrusion)

Fig. 7. Relationship between N_f and μ

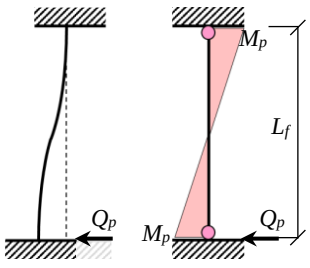

Fig. 8. Moment distribution beam when mechanism formed

Where Q_p is the horizontal load at which the mechanism is formed and K_f is the elastic stiffness. In this section, the strength and elastic stiffness are calculated by the following equations, assuming that the mechanism is formed and that the beams are fixed at both ends, respectively.

$$Q_p = \frac{2Z_p \cdot \sigma_y}{L_f} \tag{6}$$

$$K_f = \frac{12EI}{L_f^3} \tag{7}$$

In both cases, the number of fractures decreases linearly on both logarithmic axes as the plasticity factor increases. In the case of the hanging bolt (without braces) (Fig. 7(a)), the effect of the difference in length L_f is reduced by using the plasticity factor, and a uniform evaluation can be made. Similarly, the effect of the difference in the length of the lower protrusion, L_b, on the protrusion with the braces (Fig. 7(b)) is also small.

3.3 Effect of the presence or absence of threads on the low-cycle fatigue characteristics of the hanging bolt

Section 4.1 shows the fatigue characteristics of suspension support members, including a specimen in which the hanging bolt fractured in the calculated elastic range. However, even if the specimens are elastic in the calculation, they show nonlinearity due to stress concentration at the threads and other factors. In this section, the low-cycle fatigue characteristics of steel bars without threads is presented with reference to Reference [13], and the effect of the presence or absence of threads on the low-cycle fatigue characteristics of hanging bolts is discussed.

Fig. 9 shows the geometry of the test specimen in Reference [13]. The test specimen is a steel bar, consisting of a test part and a fixed part. The fixed part is tightened to the steel plate with nuts via threaded sections. The frame is consisted of four steel bars as columns, and loads are applied to the jig attached to the steel plates for cyclic loading at a constant amplitude.

The relationship between the number of fractures N_f and the deformation angle R obtained from the experiments is shown in Fig. 10, together with the results for L_b = 100 mm (three specimens with fractured bolts) in Section 4.1. The distinction between the plots in the figures is the same as in Section 4.1. The straight line in the figure is the fatigue curve for SS material shown in Ref. [13], which is expressed by the following equation using the constant deformation amplitude γ.

$$\log N_f = -1.84 \log \gamma + 3.46 \tag{8}$$

Here, the constant deformation angle γ is expressed by the following equation. In Fig.10, the constant deformation angle γ is shown by replacing it with the deformation angle R.

$$\gamma = \delta / \delta_Y \tag{9}$$

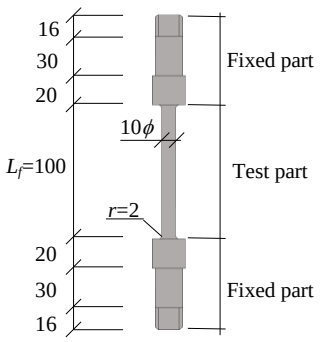

Fig. 9. Test specimen (SS-series) [13]

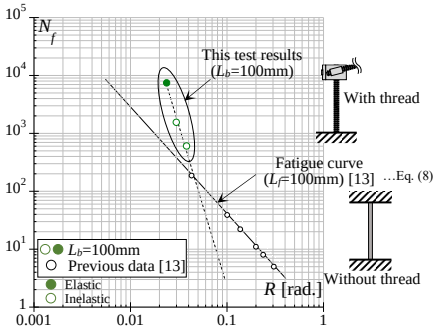

Fig. 10. Comparison of low-cycle fatigue characteristics with and without thread [13]

where δ is the one-sided amplitude applied to the specimen and δ_Y is the relative elastic horizontal deformation corresponding to the yield strength of the frame, Q_Y, calculated by the following equation.

$$\delta_Y = \frac{16\sigma_Y L_f^2}{9\pi d_0 E} \tag{10}$$

where σ_Y is the yield point (=353N/mm^2) obtained from tensile test of the specimen, L_f (=100mm) is the length of the test section, d_0 (=10mm) is the diameter of the test part, and E (=205,939N/mm^2) is Young's modulus.

The range of loading amplitude is different between this experiment and the previous experiment [13]. Comparing the fatigue curves, the unthreaded specimen [13] had fewer fractures at large amplitudes, but at small amplitudes, the relationship between the two was reversed. However, there is experimental result near the intersection of the two, and the experimental result is in general agreement with the fatigue curves of both. Therefore, it is considered that the effect of the presence or absence of threads is small in the range of loading amplitudes covered by this experiment. Detailed verification of this point is a subject for future study.

3.4 Cyclic loading test under constant amplitude (Other broken type)

This section describes the specimens in which buckling of the braces and failure of the mounting hardware were observed in the suspension support member with the shortest protrusion length (L_f = 100 mm). The relationship between the number of fractures N_f and the deformation angle R_i (i=a, b) is shown in Fig. 11. In the figure, failure due to buckling of braces is indicated by ×, and failure of mounting hardware is indicated by +. The blue plot shows the case of a lower protrusion, and the red plot shows the case of an upper protrusion. In the case of brace buckling, the experiment was finished when a significant decrease in strength was observed, and the number of cycles at that point is plotted to the figure. Failure of the mounting hardware tends to occur earlier than the fracture of the hanging bolt. The failure modes of the suspension support members confirmed in this experiment are also shown in Fig. 11. Failure of the mounting hardware tends to occur earlier than the fracture of the hanging bolt. These failures occurred at a smaller range of loading amplitudes than the one at which fatigue fracture of the

hanging bolt occurred and may be affected by the accumulation of cyclic deformation due to aftershock.

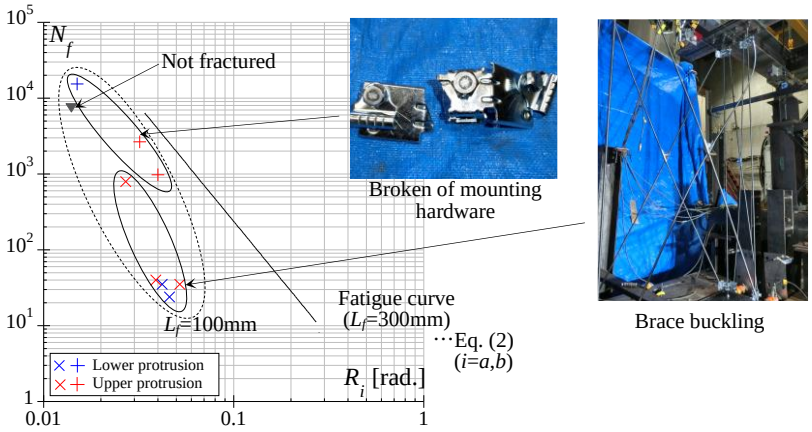

Fig. 11. Low-cycle fatigue characteristics (shown in case of other broken type)

3.5 Evaluation by cumulative damage

Next, the seismic response is assumed and the case where the loading amplitude varies over multiple amplitudes is discussed. Here, the Miner's law (linear cumulative damage rule [14]) is used to evaluate the cumulative damage (D value) of the hanging bolt. Experiments are conducted on the bolt diameter ϕ= W3/8 and the suspension length L_f =300mm (without braces). The number of fractures N_f, is calculated based on the fatigue curve of L_f =300mm without braces as shown in the equation (18) in section 4.1 and the measured deformation angle R. The loading patterns are the incremental and decremental types, and two-stage amplitude tests and three-stage amplitude tests are conducted for each. The summary of the loading pattern is shown in Fig. 12. If the number of fractures at each constant amplitude is N_{fi} and the number of cycles at each amplitude is n_i, the cumulative damage (D value) of the hanging bolt is expressed by the following equation.

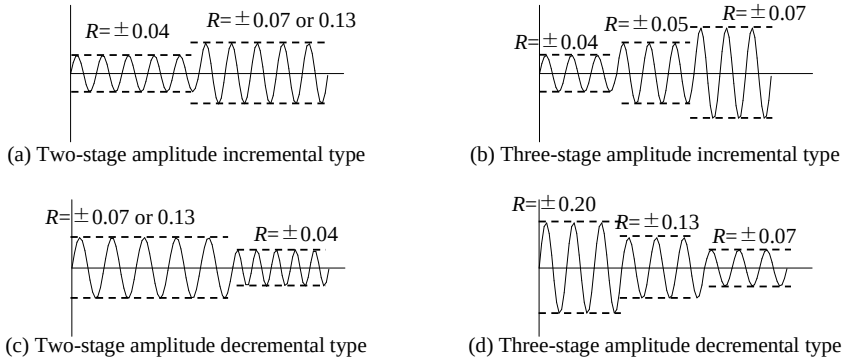

Fig. 12. Loading pattern of multi-stage amplitude test

Table 2. Cumulative damage of hanging bolt (L_f=300mm, ϕ=W3/8)

Loading pattern		φ	L [mm]	R [rad.]	N_{fi} [cycle]	n_i [cycle]	D
Incremental	Two-stage	W3/8	300	0.036	4277	4148	1.22
				0.066	741	186	
	Two-stage			0.036	4386	4148	1.37
				0.129	98	42	
	Three-stage			0.037	4165	1752	1.22
				0.048	1910	823	
				0.065	745	275	
Decremental	Two-stage			0.066	714	651	1.45
				0.037	4186	2270	
	Two-stage			0.131	94	56	1.03
				0.036	4582	1964	
	Three-stage			0.199	27	6	0.72
				0.131	93	32	
				0.064	800	126	

$$D = \sum_{i=1}^{k} \frac{n_i}{N_{fi}} \tag{11}$$

The experimental results are shown in Table 2. The D values were below 1.0 for some loading patterns, but exceeded 1.0 for many specimens, suggesting that the application of the Miner's law should be considered in the design, for example, by setting an appropriate safety factor for the fatigue curve.

4 Conclusion

In this study, cyclic loading tests of the suspension support members supporting building equipment were conducted to clarify the effects of the suspension length and the attachment angle of braces on low-cycle fatigue characteristics. The following is a summary of the results obtained.

1. It was shown that the low cycle fatigue characteristics of the hanging bolt can be evaluated independently of the presence or absence of braces by using the deformation angle at the protrusion part. The number of fractures tends to increase as the suspension length increases. This is partly because the suspension length increases, the amount of plastic deformation is relatively smaller for the same amplitude, and the use of the plasticity ratio can eliminate the effect of the difference in suspension or protrusion length L_f.
2. In the case of the suspension support members with braces and L_f=100mm, buckling of the braces and failure of the mounting hardware were observed in addition to the fracture of the hanging bolts.
3. The case where the loading amplitude is varied over several amplitudes was examined assuming an earthquake. The low-cycle fatigue characteristics of the hanging bolt was shown to be applicable to the combination of multiple amplitudes by using the Miner's law for cumulative damage.

Acknowledgement

This research was supported by Grant-in-Aid for Scientific Research (A), "Establishment of Technology for Maintain the Functionality of Interior Spaces during Earthquakes by Elucidating the Interaction between Ceilings, Walls, and Equipment" (PI: Shoichi Kishiki) and by the JSPS Fellowship for Research Fellows. We would like to express our gratitude to all the researchers who contributed to this project.

References

1. S.Taghavi, E.Miranda (2003) Response Assessment of Nonstructural Building Elements, PEER Report: 59–65.
2. Tohoku Air Conditioning and Sanitation Contractors Association (2012) Report on Damage to Equipment Cause by the Great East Japan Earthquake (in Japanese)
3. Architectural Institute of Japan (2015) Report on the Great East Japan Earthquake Disaster, Building Series Volume 8 Building Equipment and Environment, Japan. (in Japanese)
4. Earthquake Reconstruction Support Conference (2013) Equipment Damage Prevention Study Committee, Report on damage to equipment and seismic countermeasures due to the Great East Japan Earthquake (in Japanese)
5. The Building Center of Japan (2014) Guidelines for Seismic Design and Construction of Building Equipment (in Japanese)
6. The Society of Heating, Air-Conditioning and Sanitary Engineering of Japan (2023) Seismic Design and Construction Methods for Building Equipment (in Japanese)
7. Hashimoto S., Matsushita T., Miyoshi K., Tajima K., Kaneko T., Arai Y. (2014) Static Loading Test for Seismic Suspending Method of Building Equipment Part1,2. Summaries of Technical Papers of Annual Meeting, Architectural Institute of Japan, Environmental Engineering, pp.1021-1024. (in Japanese)
8. Kinoshita T., Sato Y., Aoi A., Moriyama T. (2019) Study on Fatigue Fracture of Hanging Bolt of Building Equipment. Summaries of Technical Papers of Annual Meeting, Architectural Institute of Japan, Structure-I, pp.1049-1050. (in Japanese)
9. Sakaki Y., Nishikawa T., Ohashi K., Takeda K. (2014) Study on Seismic Reinforcement and Retrofitting of Building Non-Structural Materials and Equipment Part3. AIJ Journal of Kanto Branch II. (in Japanese)
10. Noda Y., Hirano I., Kurosawa M., Kishiki S. (2023) Low-Cyclic Fatigue Characteristics of Hanging Bolt of Building Equipment Part5 Cross Sectional Characteristics of Hanging Bolt, Summaries of Technical Papers of Annual Meeting, Architectural Institute of Japan, Structure-III, pp.1053-1054. (in Japanese)
11. Hirano I., Kurosawa M., Kishiki S. (2021) Experiments on Low-cycle Fatigue Characteristics of Hanging Bolt of Building Equipment, Steel Structure Symposium, Proceeding of Constructional Steel (JSSC) Vol.29, pp.302-307. (in Japanese)
12. S.S. Manson (1961) Therman Stress and Low Cycle Fatigue, McGraw-Hill, 1966 Engineering, ASME, pp.565-571.
13. Akiyama H., Takahashi M., Shi Z. (1995) Ultimate Energy Absorption Capacity of Round-Shape Steel Rods Subjected to Bending, J. Struct. Constr. Eng., AIJ, No.475, pp.145-154 (in Japanese)
14. Miner. M.A (1945) Cumulative Damage in Fatigue Journal of Applied Mechanics, Vol.12, pp.159-164.